ChemComm

Check for updates

Gauging the donor strength of iron(0) complexes *via* their N-heterocyclic carbene gold(I) adducts†

Zhi Hao Toh,[a] Hendrik Tinnermann,[a] Dinh Cao Huan Do, [iD][a] Han Vinh Huynh, [iD][a] Tobias Krämer [iD][b] and Rowan D. Young [iD]*[a]

We isolate and characterize the gold(I)−iron(0) adducts [(ⁱPr₂-bimy)-Au−Fe(CO)₃(PMe₃)₂][BAr^F₄] and [Au−{Fe(CO)₃(PMe₃)₂}₂][BAr^F₄] (ⁱPr₂-bimy = 1,3-diisopropylbenzimidazolin-2-ylidene, BAr^F₄ = tetrakis-(pentafluorophenyl)borate). DFT analysis reveals that the gold−iron interaction in [(ⁱPr₂-bimy)Au−Fe(CO)₃(PMe₃)₂][BAr^F₄] is predominantly a σ-donation from iron to gold. We further extend this class of compounds to include [(ⁱPr₂-bimy)Au−Fe(CO)₃(PR₃)₂][BAr^F₄] (PR₃ = PPh₃, PCy₃, PCyPh₂, PMePh₂, PMe₂Ph, P(4-C₆H₄F)₃) and [(ⁱPr₂-bimy)-Au−Fe(CO)₄(PPh₃)][BAr^F₄] and correlate the ⁱPr₂-bimy carbenic ^{13}C NMR signal with the relative donor strength of the iron(0) ligand. This approach allows for a fast and simple approach to gauge relative donor strength of Fe(0) donors.
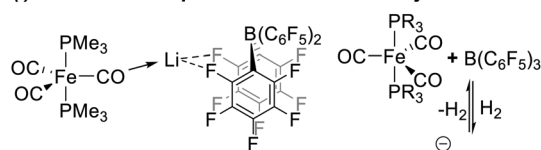
Transition metals hold a traditional role as Lewis acids in activation and coordination chemistries. However, the use of metals as bases in metal-only Lewis pair (MOLP) and frustrated Lewis pair (FLP) systems has recently become well recognized (Fig. 1).[1] Metal base partners in FLP and MOLP systems result in enhanced activity and a plethora of post-activation functionalization options that are unavailable to main-group Lewis bases. Notably, this allows the use of first row transition metals in difficult catalytic transformations that commonly rely upon noble metals.[2]

Recently, we have reported on the use [Fe(CO)₃(PR₃)] {R = Me (**1a**), Ph (**1b**), Cy (**1c**)} as Lewis bases in FLP chemistry where pronounced differences were observed based on the electron donating ability and steric profile of the phosphine substituents.[3] Iron(0) complexes have also been used extensively as donors in coordination chemistry,[1a] notably as ligands for Cu, Ag, and Au complexes.[4] However, gauging the donor strength of iron(0) (and other metal ligands) remains challenging. Previous
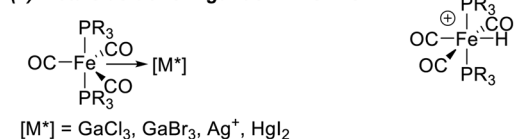
efforts to determine the basicity and/or donor strength of iron(0) complexes have been crude, unreliable and/or analytically difficult.

Braunschweig used the transfer of the Lewis acid GaCl₃ between Fe(0), Ru(0) and Pt(0) to gauge their relative Lewis basicity.[5] He also applied the method pioneered by Gandon[6] in measuring the hybridization of GaCl₃ bound to the zero valent metal adducts to infer donor strength. Such an approach is contingent upon favourable formation and isolation of the GaCl₃ adducts and their structural characterization. Additionally, such an approach may not reflect the behavior of the Fe(0) bases in solution where crystal packing effects manipulate the geometry of GaCl₃. The Brønsted basicity of a large number of metal complexes has also been determined from the pK_a of their conjugate
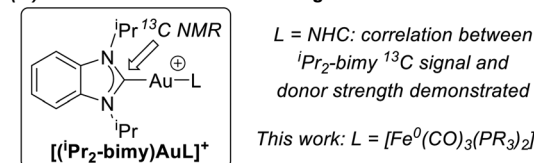

Fig. 1 (i) Zero valent iron complexes used as base partners in FLP chemistry.[3] (ii) Zero valent iron complexes acting as ligands.[5] (iii) Correlation between the carbenic ^{13}C NMR signal of ⁱPr₂-bimy in [(ⁱPr₂-bimy)AuL]⁺ and donor strength was shown for L = NHC providing a fast and accurate way to quantify the donor strength of ligands *via* NMR spectroscopy.[9] Can it be applied in an analogous manner to transition metals such as iron(0) donors?
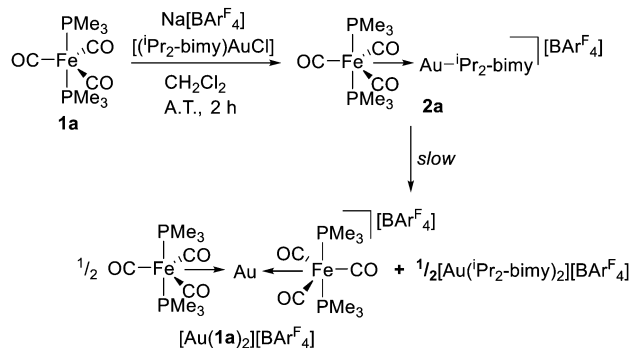
[a] *Department of Chemistry, National University of Singapore, 3 Science Drive 3, 117543, Singapore. E-mail: rowan.young@nus.edu.sg*

[b] *Department of Chemistry, Maynooth University, Maynooth, Co. Kildare, Ireland*

Scheme 1 Formation of bimetallic complex **2a** from **1a**, [(^{i}Pr$_2$-bimy) AuCl] and Na[BAr$^F_4$]. **2a** can further disproportionate into [Au(**1a**)$_2$][BAr$^F_4$] and [Au(^{i}Pr$_2$-bimy)$_2$][BAr$^F_4$].

acids (metal hydrides).[7] Most pK_a values are determined *via* equilibria with bases of known pK_b, making determination of highly acidic metal hydrides difficult. This method is also imprecise, with error as high as 20%, and widely different values can be obtained depending on which yardstick base is used in the equilibrium. Further, established means to measure main group ligand donor strengths, such as the Tolman electronic parameter (TEP), Crabtree's modified electronic parameter and the Lever electronic parameter (LEP) are inept for weak and highly reductive donors such as Fe(0) complexes.[8]

As an alternative to these methods (*e.g.* TEP, LEP) Huynh has reported on the correlation between ligand donor strengths and shift in the ^{13}C NMR signal of a spectator ligand in complexes of the type [(^{i}Pr$_2$-bimy)PdBr$_2$(L)] and [(^{i}Pr$_2$-bimy)Au(L)]$^+$ (^{i}Pr$_2$-bimy = 1,3-diisopropylbenzimidazolin-2-ylidene, see Fig. 1(iii)).[9] The ^{13}C NMR signal of the benzimidazolinylidene carbon donor in [(^{i}Pr$_2$-bimy)PdBr$_2$(L)] corresponds to the Huynh electronic parameter (HEP) (where better donor ligands lead to lower field shifts), and Huynh has shown that the ^{13}C carbenic NHC signal in [(^{i}Pr$_2$-bimy)Au(L)]$^+$ complexes can be directly correlated to the HEP for carbene ligands (this has yet to be expanded to other ligand classes). Given that Fe(0) has previously been reported to form complexes with gold fragments,[4a,b] we envisioned that the synthesis of bimetallic compounds of the type [(^{i}Pr$_2$-bimy)Au–Fe(CO)$_3$(PR$_3$)$_2$][BAr$^F_4$] {BAr$^F_4$ = tetrakis(pentafluorophenyl)borate} might allow an accurate ordering and comparison of the donor strengths of Fe(0) complexes as ligands.

To this end, we herein report on the formation and characterization of the Fe–Au adduct [(^{i}Pr$_2$-bimy)Au–Fe(CO)$_3$(PMe$_3$)$_2$][BAr$^F_4$] (**2a**). We extend this class of complexes to [(^{i}Pr$_2$-bimy)Au–Fe(CO)$_3$-(PR$_3$)$_2$][BAr$^F_4$] (PR$_3$ = PPh$_3$, PCy$_3$, PCyPh$_2$, PMePh$_2$, PMe$_2$Ph, P(4-C$_6$H$_4$F)$_3$) and find a correlation between their carbenic ^{13}C NMR signal, their pK_a and the TEP of the iron coordinated phosphine group. The ability to gauge the donor strength of iron(0) complexes (and potentially other donor metals) using this method circumvents the need to isolate unstable Fe–Au adducts and provides a high precision determination of relative Fe(0) donor strength.

Complex **2a** was formed from mixing a solution of [Fe(CO)$_3$(PMe$_3$)$_2$] (**1a**) with Na[BAr$^F_4$] and [(^{i}Pr$_2$-bimy)AuCl] in stoichiometric quantities (Scheme 1). The reaction was found to also form [Au(^{i}Pr$_2$-bimy)$_2$][BAr$^F_4$] and [Au{Fe(CO)$_3$(PMe$_3$)$_2$}$_2$][BAr$^F_4$]

([Au(**1a**)$_2$][BAr$^F_4$]), presumably *via* disproportionation of **2a**. Nonetheless, compound **2a** was found to be the predominant species formed with an NMR yield of 77% and could be isolated in 47% yield. The identity of [Au(**1a**)$_2$][BAr$^F_4$] and [Au(^{i}Pr$_2$-bimy)$_2$]- [BAr$^F_4$] were confirmed *via* independent syntheses (see ESI†). Single crystal X-ray diffraction (SCXRD) analysis of [Au(**1a**)$_2$]- [BAr$^F_4$] (Fig. 2) revealed its structure to be closely related to the silver analogue [Ag{Fe(CO)$_3$(PMe$_3$)$_2$}$_2$][BAr$^{Cl}_4$] reported by Braunschweig.[4g] It was found that isolated samples of **2a** dissolved in CH$_2$Cl$_2$ slowly formed [Au(**1a**)$_2$][BAr$^F_4$] and [Au(^{i}Pr$_2$-bimy)$_2$][BAr$^F_4$] over a matter of hours.

Spectroscopic data for **2a** reveal a decrease in the electron density and a reduction in symmetry at the iron centre, with $\nu_{(CO)}$ shifting from 1871 cm^{-1} in **1a** to 2005 cm^{-1}, 1946 cm^{-1} and 1923 cm^{-1} in **2a** (values in CH$_2$Cl$_2$ solution). And the ^{31}P NMR signal arising from the PMe$_3$ ligands shifting upfield from δ_P 38.4 in **1a** to 23.6 in **2a**. A signal at 190.1 ppm in the ^{13}C NMR spectrum of **2a** was identified as the ^{i}Pr$_2$-bimy carbenic resonance, with coupling to the iron bound PMe$_3$ ligands observable ($^3J_{PC}$ = 4.8 Hz, t, 2 P, CD$_2$Cl$_2$ solvent).

Compound **2a** could be crystallized *via* diffusion of *n*-hexane into a saturated DCM solution at room temperature to generate crystals suitable for SCXRD. The molecular structure of **2a** (Fig. 3) reveals a close Au–Fe contact at 2.562(1) Å. This distance is notably shorter than the M–Fe bond distances in [Au(**1a**)$_2$][BAr$^F_4$] (Au–Fe = 2.578(1) Å), implying a significant Au–Fe interaction in **2a**. Indeed, evidence for a strong Fe–Au interaction can also be observed through a strong *trans* influence, elongating the Au–C$_{NHC}$ distance to 2.032(3) Å. This distance is longer than Au–C$_{NHC}$ distances observed in reported [Au(^{i}Pr$_2$-bimy)(L)]$^+$ complexes with weak doners, *e.g.* pyridine {Au–C$_{NHC}$ = 1.983(5) Å}, and similar to strong donors such as NHC ligands, *e.g.* ^{i}Pr$_2$-bimy {Au–C$_{NHC}$ = 2.023(6) Å}, ^{i}Pr {Au–C$_{NHC}$ = 2.015(5) Å}.[9c]

The carbonyl environment around the iron centre in **2a** fails to adopt an octahedral geometry, as is observed in other Fe(0)→M complexes,[4] and two of the carbonyl ligands are bent towards the Au coordination site, with C–Fe–Au angles of 68.6(1)° and 73.8(1)°. Similar OC–Fe–CO geometries have been observed in Braunschweig's [Ag{Fe(CO)$_3$(PMe$_3$)$_2$}$_2$][BAr$^{Cl}_4$][4g] and group 10 [Fe(CO)$_5$] adducts,[4a,b,e,f,h] however, a DFT analysis by Frenking[4b] on [LAu–Fe(CO)$_5$]$^+$ systems (L = NHC or phosphine) concluded that there was little interaction between gold
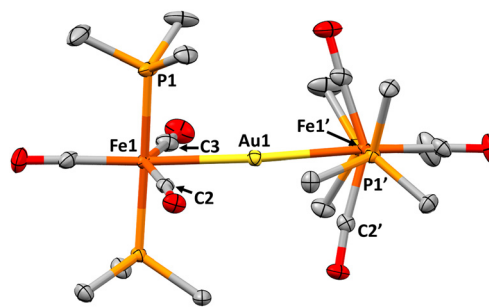
Fig. 2 Molecular structure of [Au(**1a**)$_2$][BAr$^F_4$]. Hydrogen atoms and anion omitted, thermal ellipsoids shown at 50%. Selected bond distances (Å) and angles (°): Fe1–Au1, 2.580(1); Au1–C2, 2.612(2); Fe1–Au1–Fe2, 176.4(1).
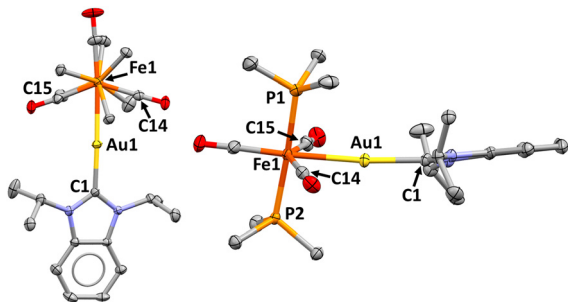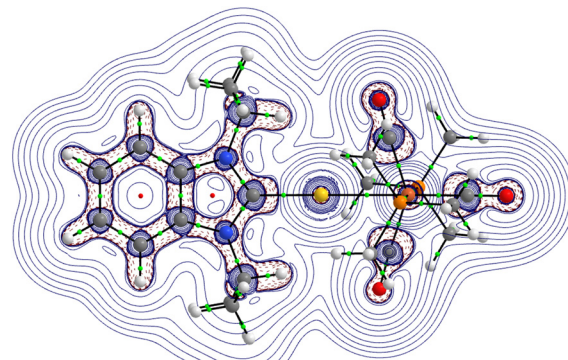
Fig. 3 Axial and equatorial perspectives for the molecular structure of **2a**. Hydrogen atoms and anion omitted, thermal ellipsoids shown at 50%. Selected bond distances (Å) and angles (°): Au1–Fe1, 2.562(1); Au1–C1, 2.031(3); Au1–C15, 2.532(3); Fe1–Au1–C1, 175.1(1); C14–Fe1–C15, 142.0(1).

Au–Fe $\rho(r_c)$ 0.331 eÅ^{-3}; $\nabla^2\rho(r_c)$ 3.133 eÅ^{-5}; $H(r_c)$ −0.061 E_hÅ^{-3}
Au–C $\rho(r_c)$ 0.877 eÅ^{-3}; $\nabla^2\rho(r_c)$ 10.411 eÅ^{-5}; $H(r_c)$ −0.378 E_hÅ^{-3}

Fig. 4 Contour plot of the Laplacian of electron density $\nabla^2(r_c)$ in the Au–Fe–C$_{(CO)}$ plane of **2a** (BP86-D3(BJ)/def2TZVPP/x2C-TZVPall). Values of key topological descriptors are also given. Blue solid lines indicate regions of charge depletion ($\nabla^2(r_c) > 0$) and red dotted lines indicate regions of charge accumulation ($\nabla^2\rho(r) < 0$). Green and red dots represent bond and ring critical points, respectively.

and the iron carbonyl ligands bent towards the gold centre despite the acute C–Fe–Au angles.

Huynh has found that HEP values correlate well to donor strength for σ-type donors, thus we aimed to understand the bonding between **1a** and the '{(^{i}Pr$_2$-bimy)Au}' fragment and whether the carbonyl groups of **1a** were involved in bonding with this fragment. To this end, we scrutinized the electronic structure of **2a** using DFT calculations. Geometry optimization at the BP86-D3/def2-TZVP(+RECP on Au)/def-SVP level reproduced experimentally observed distances and ν_{CO} for **2a** with high accuracy (Table S2, ESI†). The QTAIM analysis of the electron density does not reveal any bond critical points between Au and the in-plane CO carbon atoms, suggesting that the interaction is predominantly between Au and Fe, with little to no contribution from the carbonyl ligands (Fig. 4). Frenking's analysis of [LAu–Fe(CO)$_5$]$^+$ systems (L = NHC or phosphine) rendered a similar conclusion, with QTAIM parameters associated with **2a** similar to those in Frenking's study.[4b]

The NOCV energy decomposition of the orbital interaction further supports this conclusion (Fig. S34, ESI†). The analysis reveals a dominant σ-type donor–acceptor interaction between the Fe centre and Au$^+$ (6s/6p) with a much smaller π-interaction arising from backdonation from filled 5d AOs of Au$^+$ to vacant carbonyl ligand molecular orbitals. Again, deformation densities and their respective fragment orbitals, as well as the associated interaction strength correlate strongly to Frenking's data. The σ-type interaction is also apparent from inspection of the MO diagram, where HOMO−1 shows relatively small contribution from the in-plane CO ligands. They are involved to some extent in some backbonding (which is very weak and only the dominant contribution is shown in Fig. S35, ESI†). The remainder of the MO diagram is unsurprising, and all d orbitals associated with the Au and Fe centres can be readily identified. The character of the vacant d$_{z^2}$ of Fe^0 (d^8) is smeared out over LUMO+2 and LUMO+3. DLPNO/CCSD(T) Local Energy Decomposition Analysis suggests a substantial binding energy of 66.7 kcal mol^{-1} between the two metal fragments (Table S3, ESI†). Interestingly, almost 33% of stabilization is due to London dispersion. Natural population analysis places a positive charge of +0.67e on Au.

Given the above conclusion, we proceeded to extend the measurement of ^{13}C NMR ^{i}Pr$_2$-bimy carbenic signal values to other iron(0) complexes capable of acting as donors. To achieve this, we reacted Na[BAr$^F_{20}$], [AuCl(^{i}Pr$_2$-bimy)] and [Fe(CO)$_3$(PR$_3$)$_2$] {PR$_3$ = PPh$_3$, PCy$_3$, PCyPh$_2$, PMePh$_2$, P(4-C$_6$H$_4$F)$_3$} together in CD$_2$Cl$_2$ then proceeded to measure their characteristic ^{13}C NMR reporter signal. Huynh has established that a more positive (downfield) ^{13}C NMR reporter signal for the ^{i}Pr$_2$-bimy ligand corresponds to a better σ-donor ligand.

It can be seen that the ordering of iron(0) ligands is as would be expected, with phosphino groups with more electron-donating substituents that generate a more electron rich Fe centre providing more positive ^{13}C NMR values (Table 1). Notably, the ordering of the ^{13}C NMR reporter signals of the '(^{i}Pr$_2$-bimy)Au' fragment follows the same ordering as the conjugate acid pK_a values of the Fe(0) ligands (for those that are reported) with a strong linear relationship correlation (R^2 = 0.9612, Fig. 5). It must be noted that in many instances the desired product was not dominant and/or stable (rendering isolation challenging). However, this NMR spectroscopic approach allowed us to gauge the donor strength of complexes **1** even when the target complexes **2** were in low concentration.[10]
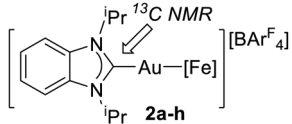
Further, we extended this technique to the tetracarbonyl iron(0) complex [Fe(CO)$_4$(PPh$_3$)] through ^{13}C NMR analysis of [(^{i}Pr$_2$-bimy)Au–Fe(CO)$_4$(PPh$_3$)][BAr$^F_4$] (**2h**). As would be expected from the substitution of a phosphine with a more π-acidic ligand (*i.e.* CO), the ^{13}C NMR reporter signal appeared at a higher field position (at 185.4 ppm), correlating with a poorer iron σ-donor. It is important to note that the high acidity of protonated [Fe(CO)$_4$L] type complexes complicates their pK_a determination,[7] although Braunschweig has successfully applied his method of GaCl$_3$ complexation to such complexes.[5]
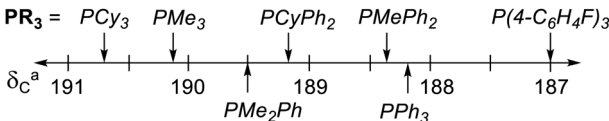
^{13}C NMR reporter signals for the '{(^{i}Pr$_2$-bimy)Au}' fragment with NHC, acyclic diamino carbene (ADC) and carbodicarbene (CDC) ligands have been reported.[9c,11] Further, we recorded the ^{13}C NMR reporter signals for [Au(^{i}Pr$_2$-bimy)$_2$][BAr$^F_4$] and [(^{i}Pr$_2$-bimy)Au(NC$_5$H$_5$)][BAr$^F_4$] to be 187.5 and 168.3 ppm respectively (Table 1). Comparison of these data to **2a** suggest

Table 1 iPr2-bimy carbenic [13C] NMR signals from complexes [(iPr2-bimy)Au–L][BArF4], Tolman electric parameter of iron phosphine ligands and pK_a values of protonated iron complexes

[Fe] donor complex	$\delta_C{}^a$	TEP[7a] of PR3	[HFe]+ pK_a[6]
Fe(CO)3(PMe3)2 (**1a**)	190.1	2064.1	3.2–4 (DCE)
Fe(CO)3(PPh3)2 (**1b**)	188.2	2068.9	−0.6 to −1.1 (DCE)
Fe(CO)3(PCy3)2 (**1c**)	190.7	2056.4	4.4 (DCE)
Fe(CO)3(PMePh2)2 (**1d**)	188.4	2067.0	0.1–1 (DCE)
Fe(CO)3(PMe2Ph)2 (**1e**)	189.5	2065.3	2.1 (DCE)
Fe(CO)3(PCyPh2)2 (**1f**)	189.2	n/a	2 (DCE)
Fe(CO)3(P(4-C6H4F)3)2 (**1g**)	187.0	2071.3	n/a
Fe(CO)4(PPh3) (**1h**)	185.4	2068.9	n/a
Main group donors (L)			[HL]+ pK_a
Pyridine		168.3	8.3 (DCM)
iPr2-bimy		187.5	n/a

^{a} [13C] NMR signal of iPr2-bimy donor atom taken in CD_2Cl_2 (solvent reference 53.84 ppm).[12]
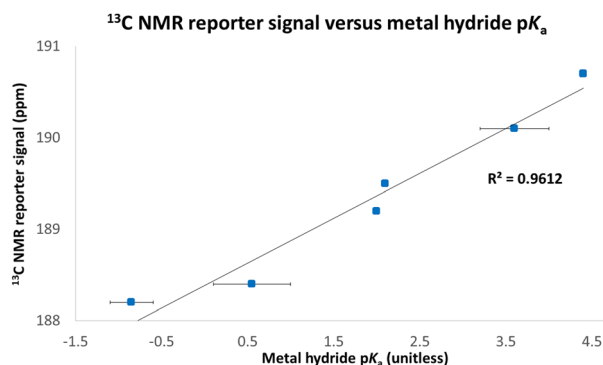
Fig. 5 Correlation between [13C] NMR reporter signal for (iPr2-bimy)Au–[Fe] complexes and the pK_a values for the conjugate acids (metal hydrides) of the Fe(0) complexes. Bars represent ranges of pK_a values where more than one report exists.

that **1a** has similar electron donation ability to NHCs on Au(I), and is a much better donor than pyridine. This is in agreement with hybridisation measurements of $GaCl_3$ bound to **1a**, NHCs and pyridine, and the large calculated Au–Fe binding energy (Table S3, ESI†).[5a,6]

In summary, we have synthesized and fully characterized the iron–gold adducts [(iPr2-bimy)Au–Fe(CO)3(PMe3)2][BArF4] (**2a**) and [Au{Fe(CO)3(PMe3)2}2][BArF4] ([Au(**1a**)2]), where [Fe(CO)3(PMe3)2] (**1a**) acts as a ligand to the gold fragment. DFT supports the description of **1a** as primarily a σ-donor to the gold centre in **2a**, with only relatively little interaction between iron–carbonyl ligands and the gold centre, despite an acute Au–Fe–CO angle observed in the molecular structure of **2a**. A

correlation was found between the apparent donor strength of iron(0) complexes of the type [Fe(CO)3(PR3)2] (PR3 = PMe3, PPh3, PCy3, PCyPh2, PMePh2, P(4-C6H4F)3) and the carbenic [13C] NMR signal of the '(iPr2-bimy)Au' fragment in complexes of the type [(iPr2-bimy)Au–Fe(CO)3(PR3)2][BArF4]. This allows for a simple method to gauge donor strength in such Fe(0) complexes, and we will be exploring if this concept can be extended to other metal ligands capable of forming adducts with gold(I).

Conflicts of interest

The authors declare no competing financial interest.

References

1 (a) J. Bauer, H. Braunschweig and R. D. Dewhurst, *Chem. Rev.*, 2012, **112**, 4329; (b) N. Hidalgo, M. G. Alférez and J. Campos, Frustrated Lewis Pairs Based on Transition Metals, in *Frustrated Lewis Pairs*, ed. C. J. Slootweg and A. R. Jupp, Springer: Cham, 2021, vol. 2, pp. 319–359.

2 (a) N. P. Mankad, Catalysis with multinuclear complexes, in *Non-noble metal catalysis molecular approaches and reactions*, ed. R. J. M. Klein Gebbink and M.-E. Moret, Wiley-VCH, Weinheim, Germany, 2019, pp. 49–68; (b) I. G. Powers and C. Uyeda, *ACS Catal.*, 2017, **7**, 936; (c) W. Xu, L. Qiao and J. Xie, *Chem. Commun.*, 2020, **56**, 8524.

3 (a) H. Tinnermann, C. Fraser and R. D. Young, *Dalton Trans.*, 2020, **49**, 15184; (b) H. Tinnermann, S. Sung, D. Csókás, Z. H. Toh, C. Fraser and R. D. Young, *J. Am. Chem. Soc.*, 2021, **143**, 10700.

4 For recent examples see: (a) G. Wang, T. T. Ponduru, Q. Wang, L. Zhao, G. Frenking and H. V. R. Dias, *Chem. – Eur. J.*, 2017, **23**, 17222; (b) S. Pan, S. M. N. V. T. Gorantla, D. Parasar, H. V. R. Dias and G. Frenking, *Chem. – Eur. J.*, 2021, **27**, 6936; (c) B. Berti, M. Bortoluzzi, C. Cesari, C. Femoni, M. C. Iapalucci, R. Mazzoni, F. Vacca and S. Zacchini, *Eur. J. Inorg. Chem.*, 2019, 3084; (d) B. Berti, M. Bortoluzzi, C. Cesari, C. Femoni, M. C. Iapalucci, R. Mazzoni, F. Vacca and S. Zacchini, *Inorg. Chem.*, 2019, **58**, 2911; (e) G. Wang, A. Noonikara-Poyil, I. Fernández and H. V. R. Dias, *Chem. Commun.*, 2022, **58**, 3222; (f) G. Wang, Y. S. Ceylan, T. R. Cundari and H. V. R. Dias, *J. Am. Chem. Soc.*, 2017, **139**, 14292; (g) H. Braunschweig, R. D. Dewhurst, F. Hupp and C. Schneider, *Chem. Commun.*, 2014, **50**, 15685; (h) P. J. Malinowski and I. Krossing, *Angew. Chem., Int. Ed.*, 2014, **53**, 13460.

5 (a) H. Braunschweig, R. D. Dewhurst, F. Hupp, C. Kaufmann, A. K. Phukan, C. Schneider and Q. Ye, *Chem. Sci.*, 2014, **5**, 4099; (b) H. Braunschweig, C. Brunecker, R. D. Dewhurst, C. Schneider and B. Wennemann, *Chem. – Eur. J.*, 2015, **21**, 19195; (c) B. Demerseman, G. Bouquet and M. Bigorgne, *J. Organomet. Chem.*, 1972, **35**, 341.

6 A. El-Hellani, J. Monot, S. Tang, R. Guillot, C. Bour and V. Gandon, *Inorg. Chem.*, 2013, **52**, 11493.

7 (a) R. H. Morris, *Chem. Rev.*, 2016, **116**, 8588; (b) R. H. Morris, *J. Am. Chem. Soc.*, 2014, **136**, 1948.

8 (a) C. A. Tolman, *J. Am. Chem. Soc.*, 1970, **92**, 2953; (b) A. R. Chianese, X. Li, M. C. Janzen, J. W. Faller and R. H. Crabtree, *Organometallics*, 2003, **22**, 1663; (c) A. B. P. Lever, *Inorg. Chem.*, 1990, **29**, 1271.

9 (a) Q. Teng and H. V. Huynh, *Dalton Trans.*, 2017, **46**, 614; (b) H. V. Huynh, Y. Han, R. Jothibasu and J. A. Yang, *Organometallics*, 2009, **28**, 5395; (c) S. Guo, H. Sivaram, D. Yuan and H. V. Huynh, *Organometallics*, 2013, **32**, 3685; (d) H. V. Huynh, *Chem. Lett.*, 2021, **50**, 1831.

10 For low concentration samples [13C] iPr2-bimy was used.

11 (a) X. Xu, Z. Zhang, S. Huang, L. Cao, W. Liu and X. Yan, *Dalton Trans.*, 2019, **48**, 6931; (b) C. Singh, A. Kumar and H. V. Huynh, *Inorg. Chem.*, 2020, **59**, 8451; (c) S.-k Liu, W.-C. Chen, G. P. A. Yap and T.-G. Ong, *Organometallics*, 2020, **39**, 4395.

12 G. R. Fulmer, A. J. M. Miller, N. H. Sherden, H. E. Gottlieb, A. Nudelman, B. M. Stoltz, J. E. Bercaw and K. I. Goldberg, *Organometallics*, 2010, **29**, 2176.